

Coarse-grained computation of traveling waves of lattice Boltzmann models with Newton–Krylov solvers

Giovanni Samaey¹, Wim Vanroose¹, Dirk Roose¹, and Ioannis G. Kevrekidis²

¹ Dept. of Computer Science, K.U. Leuven, Celestijnenlaan 200A, 3001 Leuven, Belgium

² Dept. of Chemical Engineering and PACM, Princeton University, Princeton, NJ08544

November 20, 2018

Abstract

For many complex dynamical systems, a separation of scales prevails between the (microscopic) level of description of the available model, and the (macroscopic) level at which one would like to observe and analyze the system. For this type of problems, an “equation-free” framework has recently been proposed. Using appropriately initialized microscopic simulations, one can build a coarse-grained time-stepper to approximate a time-stepper for the unavailable macroscopic model. Here, we show how one can use this coarse-grained time-stepper to compute coarse-grained traveling wave solutions of a lattice Boltzmann model. In a moving frame, emulated by performing a shift-back operation after the coarse-grained time-step, the traveling wave appears as a steady state, which is computed using an iterative method, such as Newton–GMRES. To accelerate convergence of the GMRES procedure, a macroscopic model-based preconditioner is used, which is derived from the lattice Boltzmann model using a Chapman–Enskog expansion. We illustrate the approach on a lattice Boltzmann model for the Fisher equation and on a model for ionization waves.

1 Introduction

There is an established algorithmic infrastructure to study the long-term dynamical features of systems of partial differential equations (PDEs), such as steady states or periodic solutions. When only a simulation code (a time-stepper) is available, algorithms such as the recursive projection method (RPM) [34] and Newton–Picard [24, 26] can locate steady states, as well as their stability, and perform a continuation for changing values of the parameters. These methods project the Jacobian onto the eigenspace corresponding to the slowly decaying modes, which is typically low-dimensional. In this subspace, a Newton iteration is performed; in the orthogonal complement, Picard iterations (time-stepping) converge fast enough to the steady state. Alternatively, so-called Jacobian-free Newton–Krylov methods [20] solve the linear system for each Newton correction by means of an iterative method, such as GMRES, for which an appropriate preconditioner is crucial. Both standard preconditioning techniques, such as incomplete LU factorization (ILU) and multigrid, as well as application-specific physics-based preconditioners have been proposed, see [20] for an overview and references. If required, the stability can be computed as a post-processing step [21]. As a common feature, all these methods only use selected matrix-vector products with the system’s Jacobian, which are estimated using the time-stepper with several nearby initial conditions.

Unfortunately, a low-dimensional macroscopic PDE is often not able to capture all detailed physical interactions accurately. In such cases, one needs to resort to a more microscopic description. For instance, the dynamics of a system of colliding particles with interactions that depend sensitively on the relative particle velocities can, in general, not be modeled by a reaction-diffusion equation for the particle density. One example, which forms the main motivation for the present paper, is the impact ionization reaction, where each collision of an electron with a neutral atom or molecule creates an additional electron when the relative velocity is above a certain threshold. Such a dynamical system should be modeled through a phase space evolution law, e.g. a Boltzmann equation.

Nevertheless, a clear separation in time-scales is often present in the microscopic model: on fast time-scales, the microscopic variables equilibrate with respect to a few macroscopic variables, while these macroscopic variables themselves evolve on much slower time-scales. When this is the case, a macroscopic model should conceptually exist. However, it might be difficult (or impossible) to derive a closed expression from the underlying microscopic model without introducing assumptions that are hard to justify.

For such models, there is an active current interest in the development of so-called *equation-free methods* to study the long-term behavior [19]. The key idea, which was first proposed in [38], is to construct a *coarse-grained time-stepper* for the unavailable macroscopic equation as a three step procedure: (1) lifting, i.e. the creation of appropriate initial conditions for the microscopic model, conditioned upon the macroscopic state at time t^* ; (2)

simulation, using the microscopic model, over the time interval $[t^*, t^* + \delta t]$; (3) restriction, i.e. the extraction of the macroscopic state at time $t^* + \delta t$. The result is a coarse time- δt map, which can be used to estimate the matrix-vector products that are required in an RPM, Newton–Picard or Newton–Krylov method.

Based on RPM, coarse-grained bifurcation analysis has already been used in a number of applications [17, 36], and also allows to perform other system-level tasks, such as control and optimization [35]. In this paper, we will investigate the use of Jacobian-free Newton–Krylov techniques on a model problem concerning traveling wave solutions of lattice Boltzmann models. Traveling waves are solutions that move with constant speed without changing shape; in a co-moving frame, they appear as steady state solutions. We construct a coarse-grained time-stepper in this co-moving frame by performing a shift-back operation after each coarse-grained time-step, and compute its fixed points using a Newton–GMRES procedure. To accelerate convergence of the GMRES procedure, we build a preconditioner based on an approximate PDE model, which is derived from the lattice Boltzmann model through a Chapman–Enskog expansion. As a consequence, the method described here could more appropriately be called *equation-assisted*, rather than equation-free. We expect that the techniques described here can be applied in other applications where particle based methods are necessary to describe the dynamics.

This paper is organized as follows. In section 2, we briefly review the basic properties of the coarse-grained time-stepper. Subsequently, we outline the model problems that will be used throughout the text in section 3. The non-linear system, of which the traveling waves are the solution, is constructed in section 4, and the preconditioned Newton–GMRES method is discussed in section 5. Section 6 contains a detailed numerical study of the convergence properties of the method. Finally, we conclude in section 7, which contains a discussion of the computational complexity and some final remarks.

2 Coarse-grained time-stepper

We briefly review the coarse-grained time-stepper, as it was introduced by Kevrekidis *et al.* [19]. To this end, we consider an abstract microscopic evolution law,

$$\partial_t u(\mathbf{x}, t) = f(u(\mathbf{x}, t)), \quad (1)$$

in which $u(\mathbf{x}, t)$ represents the microscopic state variables, $\mathbf{x} \in D_m$ and t are the microscopic independent variables, and ∂_t denotes the time derivative. We assume that a macroscopic model, denoted by

$$\partial_t U(\mathbf{X}, t) = F(U(\mathbf{X}, t)), \quad (2)$$

conceptually exists, but is unavailable in closed form. In equation (2), $U(\mathbf{X}, t)$ represents the macroscopic state variables, and $\mathbf{X} \in D_M$ and t are the macroscopic independent variables.

We introduce a time-stepper s for the microscopic evolution law (1),

$$u(\mathbf{x}, t + dt) = s(u(\mathbf{x}, t); dt), \quad (3)$$

where dt is the size of the microscopic time-step, and the aim is to obtain a coarse-grained time-stepper \bar{S} for the variables $U(\mathbf{X}, t)$ as

$$\bar{U}(\mathbf{X}, t + \delta t) = \bar{S}(\bar{U}(\mathbf{X}, t); \delta t), \quad (4)$$

where δt denotes the size of the coarse-grained time-step, and the bars have been introduced to emphasize the fact that the time-stepper for the macroscopic variables is only an *approximation* of a time-stepper for (2), since this equation is not explicitly known.

To define a coarse-grained time-stepper (4), we need to introduce two operators that make the transition between microscopic and macroscopic variables. We define a *lifting operator*,

$$\mu : U(\mathbf{X}, t) \mapsto u(\mathbf{x}, t) = \mu(U(\mathbf{X}, t)), \quad (5)$$

which maps macroscopic to microscopic variables, and its complement, the *restriction operator*,

$$\mathcal{M} : u(\mathbf{x}, t) \mapsto U(\mathbf{X}, t) = \mathcal{M}(u(\mathbf{x}, t)). \quad (6)$$

The restriction operator can often be determined as soon as the macroscopic variables are known. For instance, when the microscopic model consists of an evolving ensemble of many particles, the restriction typically consists of the computation of the first few low order moments of the distribution (density, momentum, energy), which are considered as the appropriate macroscopic variables $U(\mathbf{X}, t)$, in terms of which a closed macroscopic equation can be written. The assumption that a macroscopic equation closes at the level of these low order moments, implies that the higher order moments become functionals of the low order moments on time-scales which are fast compared to the overall system evolution (*slaving*).

The construction of the lifting operator is usually more involved. Again taking the example of a particle model, we need to define a mapping from a few low order moments to initial conditions for each of the particles. We know that the higher order moments of the resulting particle distribution should be functionals of the low order moments, but unfortunately, these functionals are unknown (since the macroscopic evolution law is also unknown). Several approaches have been suggested to address this problem. One could for instance initialize the higher order moments randomly. This introduces a *lifting error*, and one then relies on the separation of time-scales to ensure that the higher order moments relax quickly to a functional of the low order ones (*healing*) [14, 27, 36] (see also [30, 39]). We note that, in some cases, this approach produces inaccurate results [40]. In fact, to initialize the higher order moments correctly, one should perform a simulation of the microscopic system subject to the constraint that the low order moments are kept fixed. How this can be done using only a time-stepper for the original microscopic system, is explained and analyzed in [12, 13, 41]. We will briefly discuss the lifting step for our model problems in section 4.1.

Given an initial condition for the macroscopic variables $U(\mathbf{X}, t^*)$ at some time t^* , we can construct the time-stepper (4) in the following way:

1. **Lifting.** Using the lifting operator (5), create appropriate initial conditions $u(\mathbf{x}, t^*)$ for the microscopic time-stepper (3), consistent with the macroscopic variables.
2. **Simulation.** Use the microscopic time-stepper (3) to compute the microscopic state $u(\mathbf{x}, t)$ for $t \in [t^*, t^* + \delta t]$.
3. **Restriction.** Obtain the macroscopic state $U(\mathbf{X}, t^* + \delta t)$ from the microscopic state $u(\mathbf{x}, t^* + \delta t)$ using the restriction operator (6).

Assuming $\delta t = kdt$, this can be written as

$$\bar{U}(\mathbf{X}, t + \delta t) = \bar{S}(\bar{U}(\mathbf{X}, t), \delta t) = \mathcal{M}(s^k(\mu(\bar{U}(\mathbf{X}, t)), dt)), \quad (7)$$

where we have represented the k microscopic time-steps by a superscript on s . If the microscopic model is stochastic, one may need to perform multiple replica simulations, using an ensemble of microscopic initial conditions, to obtain an accurate result with a sufficiently low variance.

3 Model problems

We now briefly discuss the origins of the lattice Boltzmann method and the relation with the Boltzmann equation; we also introduce our model problems.

3.1 Microscopic and macroscopic model

We consider systems that, on a molecular level, consist of particles whose position and velocity are governed by two processes: free flight and collisions. We introduce the probability $f(x, v, t)dx dv$, which represents the fraction of particles with position and velocity in the infinitesimal domain $[x, x + dx] \times [v, v + dv]$ at time t . The evolution of f is governed by a so-called kinetic equation,

$$\partial_t f(x, v, t) + v\partial_x f(x, v, t) + F\partial_v f(x, v, t) = Q(f, f), \quad (8)$$

where $Q(f, f)$ is the *collision integral*, and F is an external force term. The first equation of this type was the *Boltzmann equation* for moderately rarefied gas flows with $F \equiv 0$ [2]. Of course, when multiple species are present, (8) becomes a system of equations. Throughout this paper, we confine ourselves to problems in one space dimension.

Usually, one introduces a *kinetic model* for $Q(f, f)$ to simplify equation (8) [15]. A standard choice is the non-linear Bhatnagar–Gross–Krook model (BGK) [1],

$$\partial_t f(x, v, t) + v\partial_x f(x, v, t) + F\partial_v f(x, v, t) = -\frac{f(x, v, t) - f^{eq}(x, v, t)}{\tau}. \quad (9)$$

Here, the collisions are interpreted as a relaxation to local equilibrium distribution, with a characteristic relaxation time τ . The choice of the equilibrium distribution $f^{eq}(x, v, t)$ (and therefore of the collision integral $Q(f, f)$) determines the physics of the system.

Although the kinetic equation (8) and its BGK-approximation are able to describe the evolution of a wide range of physical systems, a numerical simulation quickly becomes intractable because of the high dimensionality. However, one can often obtain an approximate macroscopic description. We define the *moments* of the distribution function as

$$\bar{\rho}^{(i)}(x, t) = m \int_{-\infty}^{\infty} v^i f(x, v, t) dv, \quad i = 0, 1, 2, \dots, \quad (10)$$

where m is the particle mass. The lowest order moments correspond to the density ($i = 0$), momentum ($i = 1$) and energy ($i = 2$), which we write as

$$\rho(x, t) = \bar{\rho}^{(0)}(x, t), \quad \phi(x, t) = \bar{\rho}^{(1)}(x, t), \quad \xi(x, t) = \bar{\rho}^{(2)}(x, t)/2. \quad (11)$$

Using the assumption that the deviation from local equilibrium is sufficiently small, one performs an asymptotic expansion (the Chapman–Enskog expansion, [22]) to obtain a closed description for the evolution of a number of low order moments. If we define the macroscopic variables as $U(x, t) = \{\bar{\rho}^{(i)}(x, t)\}_{i=0}^M$, we obtain an approximate PDE of the form

$$\partial_t U(x, t) = F\left(U(x, t), \partial_x U(x, t), \dots, \partial_x^d U(x, t)\right), \quad (12)$$

which depends on the first d spatial derivatives. Equation (12) is a good approximation of the system dynamics when there is a fast decay of the higher order terms in the Chapman–Enskog expansion.

Consider as an example the advection-diffusion equation,

$$\partial_t \rho(x, t) + c \partial_x \rho(x, t) = \partial_x (D \partial_x \rho(x, t)), \quad (13)$$

with transport coefficient c and diffusion coefficient D . This equation can be derived from equation (9) with $F \equiv 0$ by defining the equilibrium distribution as

$$f^{eq}(x, v, t) = \rho(x, t) \sqrt{\frac{\lambda}{\pi}} \exp(-\lambda(v - c)^2),$$

with $\lambda = m/2kT$, where T is temperature and k is the Boltzmann constant, and adding the conservation constraint

$$\int_{-\infty}^{\infty} (f(x, v, t) - g(x, v, t)) dv = 0.$$

A straightforward derivation reveals that the macroscopic behaviour of (9) is described by equation (13) when we choose $\tau = 2D\lambda$ [44]. Different equilibrium distributions can be used to obtain the Burgers' equation, the Euler equations, the Navier–Stokes equations, etc. One can also add chemical reactions in the collision integral [15].

In this paper, we will use the *lattice Boltzmann method* (LBM) [4, 37], which can be viewed as a special discretization of the Boltzmann equation [16]. In an LBM method, the distribution function $f(x, v, t)$ is discretized on a space-time lattice with grid spacing dx in space and dt in time. Only a discrete number of velocities are considered, which correspond to a movement over an integer number of lattice points during one time-step,

$$v_i = c_i \frac{dx}{dt}, \quad c_i = -q, -q + 1, \dots, q - 1, q.$$

For ease of exposition, we restrict ourselves to the case $q = 1$, which gives only three speeds (the so-called D1Q3 model).

For reaction-diffusion systems, we can write the evolution law for $f_i(x, t) = f(x, v_i, t)$ as

$$f_i(x + c_i dx, t + dt) = (1 - \omega) f_i(x, t) - \omega f_i^{eq}(x, t) + R_i(x, t), \quad i = -1, 0, 1. \quad (14)$$

The right-hand side approximates the collision operator, and is composed of a reaction term $R_i(x, t)$ and a BGK relaxation to the local equilibrium. After collision, the post-collision values are propagated to a neighboring lattice site, which corresponds to free flight.

For the lattice Boltzmann discretization, we can define the (non-dimensional) moments of the distribution function as

$$\rho(x, t) = \sum_{i=-1}^1 f_i(x, t), \quad \phi(x, t) = \sum_{i=-1}^1 c_i f_i(x, t), \quad \xi(x, t) = \frac{1}{2} \sum_{i=-1}^1 c_i^2 f_i(x, t). \quad (15)$$

It can easily be verified [5, 29] that, under suitable smoothness assumptions, the system is well approximated by a macroscopic reaction-diffusion equation

$$\partial_t \rho(x, t) = \partial_x (D \partial_x \rho(x, t)) + r(\rho(x, t)), \quad (16)$$

which can again be derived from the LBM equation using a Chapman–Enskog expansion [4, 42] using

$$\omega = \frac{2}{1 + 3Ddt/dx^2}, \quad R_i(x, t) = \frac{dt}{3} r(\rho(x, t)), \quad f_i^{eq}(x, t) = \rho(x, t)/3. \quad (17)$$

To view these models in the equation-free context, we define

$$u(\mathbf{x}, t) = u(x, t) = \{f_i(x, t)\}_{i=-1}^1, \quad U(\mathbf{X}, t) = U(x, t) = \rho(x, t).$$

3.2 Model problems and traveling waves

In this paper, we propose a numerical method to compute coarse-grained traveling wave solutions of lattice Boltzmann models of the form (14). Traveling waves are solutions of the form

$$U(x, t) = U(x - ct) = U(\zeta), \quad \lim_{\zeta \rightarrow \pm\infty} U(\zeta) = U_\infty^\pm, \quad (18)$$

where $\zeta = x - ct$. They appear as steady states in a moving frame (ζ, t) .

In this work, we consider traveling fronts, for which $U_\infty^- \neq U_\infty^+$. For these solutions, the evolution of the density is not sufficiently well described by the approximate reaction-diffusion PDE (16), due to a lack of smoothness of the density in the reaction front. Nevertheless, we also observe in this case that the higher order moments (momentum and energy) become (more complicated) functionals of the density on fast time-scales. As a consequence, a PDE for the density should still exist.

We consider two model problems: a model which is derived from the Fisher PDE, and a lattice Boltzmann model for ionization. Both model problems exhibit traveling fronts with arbitrary speed $c \geq c^*$, where c^* is called the critical speed.

Model problem 3.1 (Fisher model). We consider the reaction-diffusion lattice Boltzmann model,

$$f_i(x + c_i dx, t + dt) = (1 - \omega)f_i(x, t) - \omega f_i^{eq}(x, t) + R_i(x, t), \quad (19)$$

where $i = -1, 0, 1$, with

$$R_i(x, t) = \frac{dt}{3}\rho(x, t)(1 - \rho(x, t)). \quad (20)$$

Following the reasoning of the previous section, we define the approximate macroscopic PDE,

$$\partial_t \rho(x, t) = \partial_x (D \partial_x \rho(x, t)) + \rho(x, t)(1 - \rho(x, t)), \quad (21)$$

which was originally proposed by Fisher as a model for the spread of advantageous genes [11]. This equation appears in a range of physical and biological applications exhibiting waves, see e.g. [28], and supports traveling fronts of the form $\rho(x, t) = \rho(\zeta)$, with

$$\lim_{\zeta \rightarrow -\infty} \rho(\zeta) = 1, \quad \lim_{\zeta \rightarrow \infty} \rho(\zeta) = 0.$$

This model problem can be put in the equation-free framework by identifying

$$u(\mathbf{x}, t) = u(x, t) = \{f_i(x, t)\}_{i=-1}^1, \quad U(\mathbf{X}, t) = U(x, t) = \rho(x, t).$$

The Fisher equation is arguably the simplest model problem that exhibits traveling waves of arbitrary speed. It is known for the corresponding PDE that traveling waves exist with speed $c \geq c^* = 2\sqrt{D}$. Numerically, traveling waves exist for all c . However, the critical speed c^* is the lowest speed for which the traveling waves are uniformly positive. The coarse-grained traveling wave with minimal speed $c^* = 2\sqrt{D}$ is shown in figure 1.

Model problem 3.2 (Planar streamer fronts). Streamers are sharp, non-linear waves of electrons that propagate through gases in the presence of strong electric fields. The strong field accelerates the electrons that cause ionization reactions during the collisions with the neutral gas particles. This ionization reaction creates additional electrons that are, again, accelerated. This results in an avalanche at the tip of the wave front.

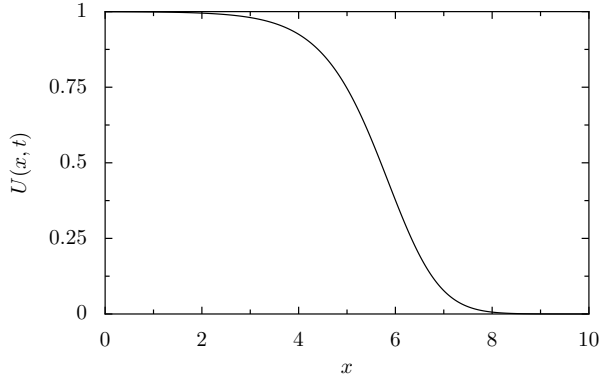


Figure 1: Coarse-grained traveling wave solution of the Fisher lattice Boltzmann model (19)-(20).

We consider a lattice Boltzmann model for the distributions $f_i(x, t)$ of electrons, which is coupled to a PDE that governs the evolution of the electric field through the electron density $\rho(x, t) = \sum_i f_i(x, t)$. The coupled equations are

$$\begin{cases} f_i(x + c_i dx, t + dt) &= (1 - \omega)f_i(x, t) - \omega f_i^{eq}(x, t) - E(x, t) \sum_j V_{ij} f_j(x, t) + R_i(x, t), \\ \partial_t E(x, t) &= -\rho(x, t)E(x, t) - D\partial_x \rho(x, t) \end{cases} \quad (22)$$

in which the electric field $E(x, t)$ appears as an external force. In the original Boltzmann equation (8), this force appears as $E(x, t)\partial_v f(x, v, t)$; in the lattice Boltzmann equation, this external force is discretized as $E(x, t)\sum_j V_{ij} f_j$, as proposed by Luo [23].

In general, the reaction terms $R_i(x, t)$ should be modeled on a microscopic level. However, due to reasons of computational complexity, most analysis of streamers is based on the Townsend approximation of the microscopic ionization reactions that appear at the tip of the front [9]. The reaction terms are then given by $R_i(x, t) = dt\rho(x, t)g(E(x, t))/3$, with $g(E) = |E|\exp(-1/|E|)$.

In this paper, we will also use this Townsend approximation to analyze the performance of our numerical method. In a forthcoming publication, the method presented here will be used to analyze the traveling waves of a five-speed lattice Boltzmann model, which is based on a more realistic set of microscopic interactions [43].

Again, we can derive an approximate PDE model,

$$\begin{cases} \partial_t \rho(x, t) = \partial_x(\rho(x, t)E(x, t)) + D\partial_x^2 \rho(x, t) + \rho(x, t)g(E(x, t)), \\ \partial_t E(x, t) = -\rho(x, t)E(x, t) - D\partial_x \rho(x, t), \end{cases} \quad (23)$$

This coupled equation exhibits traveling wave solutions with arbitrary speed $c \geq c^* = \lim_{x \rightarrow \infty} |E(x)| + 2\sqrt{Dg(E(x))}$, see figure 2.

This model problem can be put in the equation-free framework by considering

$$u(\mathbf{x}, t) = u(x, t) = \{ \{f_i(x, t)\}_{i=-1}^1, E(x, t) \}, \quad U(\mathbf{X}, t) = U(x, t) = \{ \rho(x, t), E(x, t) \}.$$

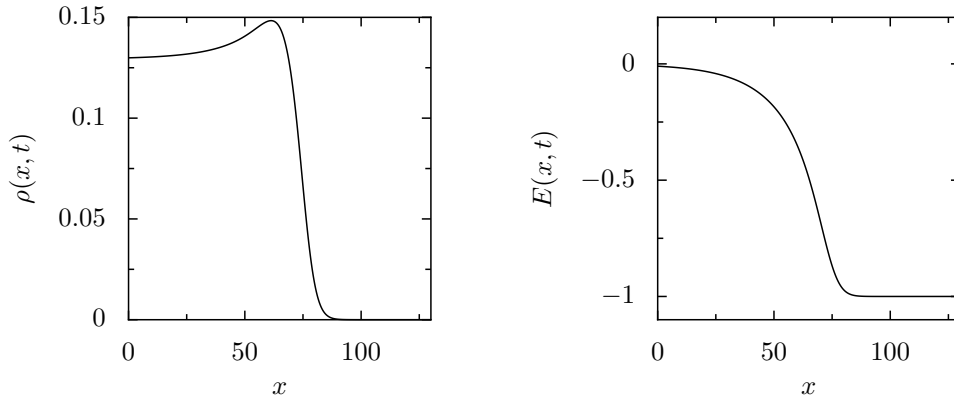


Figure 2: Coarse-grained traveling wave solution of the lattice Boltzmann model for planar streamer fronts (22). We show both the density $\rho(x, t)$ (left) and the electrical field $E(x, t)$ (right).

4 The fixed point problem

To define the fixed point problem for the traveling wave, we first construct a coarse-grained time-stepper for the lattice Boltzmann model of the form

$$\bar{U}(x, t + \delta t) = \bar{S}(\bar{U}(x, t), \delta t), \quad (24)$$

where the coarse-grained time-step $\delta t = kdt$, see equation (4). In section 4.1, we describe the details of the lifting operator.

Traveling waves appear as a one-parameter family of solutions: together with $\bar{U}^*(\zeta)$, any translate $\bar{U}^*(\zeta + \varphi)$, for an arbitrary but fixed φ , is also a traveling wave. We therefore add a phase condition to remove this indeterminacy. The specific implementation of the shift-back operator and the phase condition are discussed in section 4.2.

Note that we consider model problems for which a traveling wave exists for arbitrary $c \geq c^*$. It is of physical interest to study how the critical speed c^* depends on the system parameters. However, in this paper we confine ourselves to the computation of a traveling wave for a fixed speed c . A detailed analysis of the physical properties of the ionization model can be found in [43].

4.1 Lifting for lattice Boltzmann models

As already outlined in section 2, a coarse-grained time-stepper is constructed as a lift-simulate-restrict procedure. While the restriction step is well defined by equation (15), the lifting step can be defined in multiple ways. We discuss three possibilities.

Weighted lifting. A first possibility is to simply initialize the distributions as

$$f_i(x, t) = w_i \rho(x, t), \quad \sum_i w_i = 1, \quad (25)$$

where $w_i = 1/3$ is an obvious choice, since this corresponds to the local diffusive equilibrium as defined in equation (17). As a consequence, the higher order moments are initialized as

$$\phi(x, t) = 0, \quad \xi(x, t) = \rho(x, t)/3.$$

This very rough approximation of the higher order moments introduces a *lifting error*, and one relies on the separation of time-scales between low order and high order moments to *heal* this error quickly [38]. In [40], it is shown how this initialization can produce undesired artifacts for lattice Boltzmann models when δt is small.

Slaving relations. From the assumption that a macroscopic model for $\rho(x, t)$ exists, it follows that the higher order moments $\phi(x, t)$ and $\xi(x, t)$ can be written as functionals of $\rho(x, t)$. For lattice Boltzmann models of the form (14) with (17), these so-called *slaving relations* can be written down analytically as an asymptotic expansion in $1/\omega$. Up to third order, we have [41],

$$\begin{aligned} \phi(x, t) &= -\frac{2dx}{3\omega} \partial_x \rho(x, t) + \frac{dxdt}{\omega^2} \left(\frac{\omega}{\omega - 2} + \frac{1}{3} \right) (\partial_x r(\rho(x, t)) - \partial_{xt}^2 \rho(x, t)), \\ \xi(x, t) &= \frac{1}{3} \rho(x, t) - \frac{dt}{6\omega} (r(\rho(x, t)) - \partial_t \rho(x, t)). \end{aligned} \quad (26)$$

These expansions can alternatively be written down in terms of $\rho(x, t)$ and its spatial derivatives only, by making use of (16). The weighted lifting scheme coincides with the zeroth order term of the slaving relations.

Constrained runs scheme. Although ideally one would like to use the slaving relations to initialize the lattice Boltzmann time-stepper, this is not always possible. The analytical derivation is cumbersome, and might even be impossible when the lattice Boltzmann model is coupled to a PDE, as in model problem 3.2. Moreover, the number of higher order moments increases when a more detailed discretization of the velocity space is used. Finally, the analytic derivation of the slaving relations is only tractable if only a small number of terms of the asymptotic expansion are needed. However, the macroscopic equation becomes invalid precisely when a large number of terms is needed.

As an alternative, one can use the constrained runs scheme [12, 13] to approximate the full microscopic state corresponding to a set of predefined macroscopic variables. The idea is to perform a number of lattice Boltzmann time-steps using equation (19), where after each time-step the density is reset to the initial density. During this iteration the microscopic variables converge towards their relaxed values; correspondingly, the higher order moments have then approximately reached the slaved state. As such, the constrained runs scheme is a fixed point iteration for the higher order moments of the microscopic model. We reproduce the schematic representation that was given in [41] (figure 3).

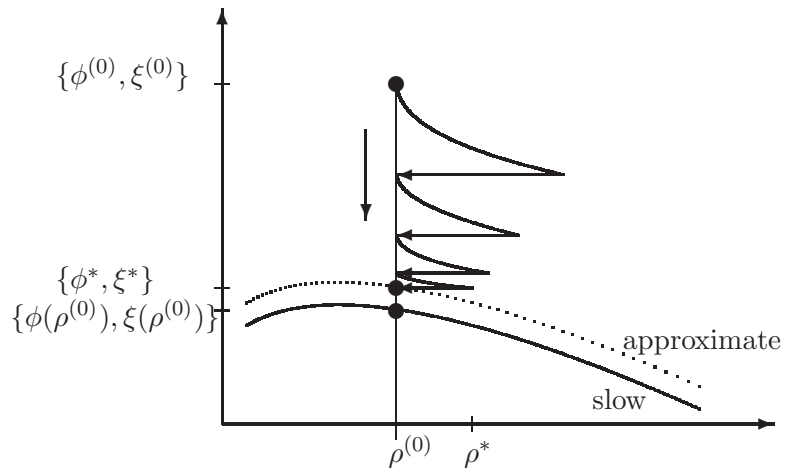


Figure 3: Sketch of the evolution of the constrained runs scheme. We plot the higher order moments ϕ and ξ as a function of the density ρ . After each lattice Boltzmann step, ρ is reset to the given $\rho^{(0)}$. The successive iterates converge to $\{\phi^*, \xi^*\}$, which is an approximation to the slaved state $\{\phi(\rho^{(0)}), \xi(\rho^{(0)})\}$ as given by equation (26). Figure reproduced from [41].

The constrained runs scheme can readily be applied to any lattice Boltzmann model, and defines a lifting operator that initializes the microscopic variables very close to their relaxed values. We refer to [41] for a detailed convergence and error analysis for reaction-diffusion systems.

4.2 Shift-back procedure and phase condition

Next, we discuss our specific implementation of the shift-back operator σ_φ . By noting that a shift-back over a distance φ is equivalent with a time evolution of the transport equation

$$\partial_t U(x, t) - \partial_x U(x, t) = 0,$$

over a time φ , we obtain

$$\sigma_\varphi : U(x, t) \mapsto \sigma_\varphi(U(x, t)) = U(x, t) + \varphi \partial_x U(x, t), \quad (27)$$

which is a valid approximation for shift-backs over short distances.

At this point, we have constructed a non-linear system

$$\bar{U}(\zeta) - \sigma_{c\delta t}(\bar{S}(\bar{U}(\zeta), \delta t)) = 0, \quad (28)$$

Unless we add a phase condition, this system is singular. When defining the Jacobian of the coarse-grained time-stepper as

$$\bar{L}(\bar{U}(\zeta), \delta t) = \frac{\partial [\sigma_{c\delta t}(\bar{S}(\bar{U}(\zeta), \delta t))]}{\partial \bar{U}(\zeta)},$$

this singularity appears as a zero eigenvalue of $I - \bar{L}(\bar{U}^*(\zeta), \delta t)$, with eigenfunction $d\bar{U}^*(\zeta)/d\zeta$.

To compensate for the extra phase condition, we add a regularization parameter α as an additional unknown, similar to what is done in [33] for Hamiltonian systems. The resulting non-linear system is

$$G(\bar{U}, \alpha) = \begin{cases} \bar{U} - \sigma_{c\delta t} (\bar{S}(\bar{U}, \delta t)) + \alpha d_{\zeta} \bar{U} & = 0, \\ p(\bar{U}) & = 0, \end{cases} \quad (29)$$

where \bar{U} denotes the space discretization of $\bar{U}(\zeta)$ and $p(\bar{U})$ is the phase condition defined below. This problem is well-posed for the unknowns (\bar{U}, α) with a locally unique solution $(\bar{U}^*, \alpha^* = 0)$.

Here, we use the phase condition

$$p(\bar{U}) = \int_{\zeta_0}^{\zeta_{N-1}} \bar{U}(\zeta) d_{\zeta} \bar{U}_{ref}(\zeta) d\zeta,$$

which minimizes phase shift with respect to the reference solution $\bar{U}_{ref}(\zeta)$, as is done in publicly available software for bifurcation analysis, such as AUTO (for ordinary differential equations) [6, 7, 8] or DDE-BIFTOOL [10] (for delay differential equations).

5 Preconditioned Newton–GMRES

We solve the non-linear equation (29) for the traveling wave solution. First, we discretize $\bar{U}(\zeta)$ on the lattice Boltzmann grid $[x_0, x_1 = x_0 + dx, \dots, x_{N-1}]$, and provide the time-stepper with homogeneous Neumann boundary conditions. The spatial derivative in (27) is discretized using central differences.

We solve the resulting non-linear system (29) with a Newton–Raphson procedure

$$\begin{cases} \bar{U}^{(k+1)} & = \bar{U}^{(k)} + d\bar{U}^{(k)}, \\ \alpha^{(k+1)} & = \alpha^{(k)} + d\alpha^{(k)}, \end{cases} \quad (30)$$

where $d\bar{U}^{(k)}$ and $d\alpha^{(k)}$ are the corrections calculated each iteration by solving linear systems of the form

$$A(\bar{U}^{(k)}, \delta t) \begin{bmatrix} d\bar{U}^{(k)} \\ d\alpha^{(k)} \end{bmatrix} = \begin{bmatrix} I - \bar{L}(\bar{U}^{(k)}, \delta t) & d_{\zeta} \bar{U}^{(k)} \\ d_{\bar{U}} p(\bar{U}^{(k)}) & 0 \end{bmatrix} \begin{bmatrix} d\bar{U}^{(k)} \\ d\alpha^{(k)} \end{bmatrix} = -G(\bar{U}^{(k)}, \alpha^{(k)}), \quad (31)$$

where $A(\bar{U}^{(k)}, \delta t)$ denotes the linearization of $G(\bar{U}, \alpha)$ around the point $(\bar{U}^{(k)}, \alpha^{(k)})$. The right hand side is the residual at the same point.

We do not have an explicit formula for $\bar{L}(\bar{U}^{(k)}, \delta t)$, since it involves the Jacobian of the coarse-grained time-stepper with shift-back. However, we can estimate matrix-vector products as

$$(I - \bar{L}(\bar{U}, \delta t)) v \approx v - \frac{\sigma_{c\delta t} (\bar{S}(\bar{U} + \epsilon v, \delta t)) - \sigma_{c\delta t} (\bar{S}(\bar{U}, \delta t))}{\epsilon}. \quad (32)$$

Therefore, we solve the linear system (31) using a Krylov method, such as GMRES [32].

The convergence rate of GMRES depends sensitively on the spectral properties of the system matrix in equation (31). For GMRES to converge rapidly, the eigenvalues should be clustered, e.g. around one [31]. It can be checked that the bordering row and column transform the zero eigenvalue of the Jacobian of (28) into $\pm\sqrt{d_{\bar{U}}p \cdot d_{\zeta}\bar{U}}$, while leaving the other eigenvalues unaltered [25]. The eigenvalues μ_k of $1 - \bar{L}(\bar{U}, \delta t)$ are of the form

$$\mu_k = 1 - \exp(\lambda_k \delta t),$$

where $\lambda_k \approx O(-k^2)$ for $k \gg 1$. For k small, $\lambda_k \approx 0$. When the system possesses a low-dimensional inertial manifold, one can choose δt large, such that the spectrum becomes a compact perturbation of the unit matrix [18]. In this case, GMRES is known to converge very quickly; this, however, at the cost of a long simulation time for each matrix-vector product. If δt is chosen to be small, the eigenvalues μ_k range from 0 to 1. In that case, preconditioning will be necessary.

We define a preconditioning matrix $M(\bar{U}, \delta t)$, and replace the linear system (31) with

$$M(\bar{U}^{(k)}, \delta t)^{-1} A(\bar{U}^{(k)}, \delta t) \begin{bmatrix} d\bar{U}^{(k)} \\ d\alpha^{(k)} \end{bmatrix} = -M(\bar{U}^{(k)}, \delta t)^{-1} G(\bar{U}^{(k)}, \alpha^{(k)}). \quad (33)$$

Ideally, $M(\bar{U}, \delta t)$ is both a good approximation of the system matrix, as well as a matrix for which an efficient (direct) solver is available. We will use a time-stepper for the approximate macroscopic equation (12) to construct $M(\bar{U}, \delta t)$. Consider the macroscopic equation (12) in the moving frame (ζ, t) ,

$$\begin{aligned} \partial_t U(\zeta, t) &= F\left(U(\zeta, t), \partial_{\zeta} U(\zeta, t), \dots, \partial_{\zeta}^d U(\zeta, t)\right) + c \partial_{\zeta} U(\zeta, t), \\ &= \tilde{F}(U(\zeta, t)). \end{aligned} \quad (34)$$

We construct a central finite difference/backward Euler time-stepper for (34) as

$$U(t + \delta t) = S(U(t), \delta t) = [I - \delta t J(U(t))]^{-1} U(t), \quad (35)$$

where again $U(t)$ is the space discretization of $U(\zeta, t)$ on the lattice Boltzmann grid, and

$$J(U(t)) = \frac{\partial \tilde{F}(U(t))}{\partial U}.$$

We then define

$$M(\bar{U}, \delta t) = \begin{bmatrix} I - (I - \delta t J(\bar{U}))^{-1} & d_{\zeta} \bar{U} \\ d_{\bar{U}} p(\bar{U}) & 0 \end{bmatrix}, \quad (36)$$

with which we will solve linear systems of the form

$$M(\bar{U}, \delta t) \begin{bmatrix} d\bar{U} \\ d\alpha \end{bmatrix} = \begin{bmatrix} b_{\bar{U}} \\ b_{\alpha} \end{bmatrix}. \quad (37)$$

The first N equations can be simplified through some algebraic manipulation,

$$\begin{aligned} & \left[I - (I - \delta t J(\bar{U}))^{-1} \right] d\bar{U} + d\alpha \cdot d_\zeta \bar{U} = b_{\bar{U}}, \\ d\bar{U} &= (I - \delta t J(\bar{U}))^{-1} d\bar{U} + b_{\bar{U}} - d\alpha \cdot d_\zeta \bar{U}, \\ d\bar{U} &= (I - \delta t J(\bar{U}))^{-1} d\bar{U} + \tilde{b}_{\bar{U}}, \\ (I - \delta t J(\bar{U})) d\bar{U} &= d\bar{U} + (I - \delta t J(\bar{U})) \tilde{b}_{\bar{U}}, \\ \delta t J(\bar{U}) d\bar{U} &= - (I - \delta t J(\bar{U})) \tilde{b}_{\bar{U}}, \end{aligned}$$

which leads to the equivalent linear system

$$\begin{bmatrix} \delta t J(\bar{U}) & - (I - \delta t J(\bar{U})) d_\zeta \bar{U} \\ d_{\bar{U}} p(\bar{U}) & 0 \end{bmatrix} \begin{bmatrix} d\bar{U} \\ d\alpha \end{bmatrix} = \begin{bmatrix} - (I - \delta t J(\bar{U})) b_{\bar{U}} \\ b_\alpha \end{bmatrix}, \quad (38)$$

in which the system matrix is the sum of a band and a rank one matrix. There exist efficient (order N) direct solvers for linear systems of this type, see e.g. [3].

6 Numerical results

6.1 Fisher equation

We consider the model problem 3.1 on the domain $[0, L]$ with $L = 10$ and with diffusion coefficient $a = 0.1$, and grid parameters $dx = 2.5 \cdot 10^{-2}$ and $dt = 1 \cdot 10^{-3}$. For these parameters $N = 400$ and $\omega \approx 1.35$. We intend to find the traveling wave with minimal speed $c^* = 2\sqrt{D}$, which is depicted in figure 1. The initial guess $\bar{U}^{(0)}$ for the Newton process is obtained by a time integration of the Fisher PDE (21) over a time interval of size $9000dt$ with initial condition

$$U(x, 0) = \rho(x, 0) = \exp(-5x^4), x \in [-L, L], \quad (39)$$

from which we take the part where $x \geq 0$.

In order to choose an adequate value for the coarse-grained time-step δt , we first illustrate the effects of the lifting operator. We then investigate the spectrum of the linear system that we need to solve, along with the effect of the preconditioner, and we conclude by showing the convergence of the Newton process.

6.1.1 Initialization

To understand the details of the initialization, we compare the exact evolution of the Fisher lattice Boltzmann model with the evolution after re-initialization. We perform an initial simulation of 100 steps with the lattice Boltzmann model, starting from the initial condition

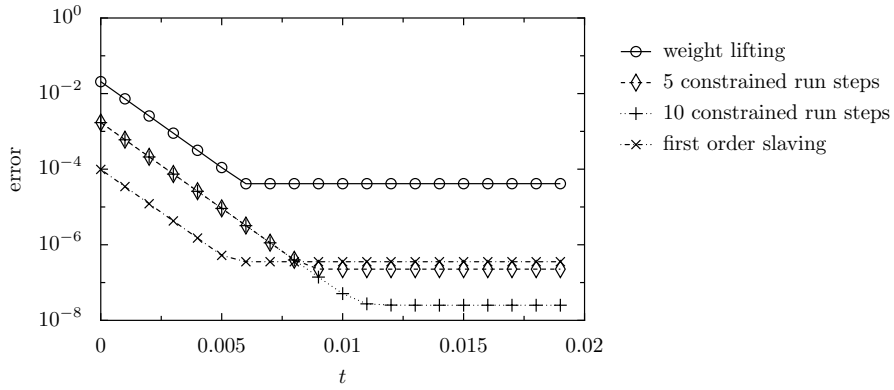


Figure 4: Evolution of the initialization error for the Fisher problem for different lifting procedures. We show the difference between the distribution function of the re-initialized and the original lattice Boltzmann simulation.

$\bar{U}^{(0)}$, which is lifted to distribution functions using the first order slaving relations. We extract the density at $t = 80dt$ using equation (15). With this density, we initialize a second lattice Boltzmann simulation using the three procedures described in section 4.1. For the slaving relations, we only use the first order approximation. We then compare the evolution of the distribution functions with the evolution of the original simulation as we continue to evolve both. The result is somewhat unexpected.

In figure 4, we plot the error between the original solution and the re-initialized simulation in the first 20 time-steps after re-initialization. We see that, in line with the results reported in [41], both the constrained runs scheme and initialization using first order slaving relations lead to a reduced lifting error, compared to weighted lifting. Unexpectedly, however, we observe that *after* initialization, all re-initialized simulations show an initial convergence towards the exact solution with a convergence rate of $|1 - \omega|$. This convergence stagnates after approximately 10 time-steps for this choice of ω . This behaviour is not completely understood yet. As is to be expected, the smallest error is obtained by fully converged constrained runs.

These results suggest that the simulation phase of the coarse-grained time-stepper, which involves the evolution of the lattice Boltzmann model from t^* to $t^* + \delta t$ requires a coarse-grained time-step δt that is at least 10 times the microscopic time-step dt to eliminate initial transients caused by the lifting for this choice of ω . If a shorter time is chosen, undesired artifacts will show up in the spectrum of the coarse-grained time stepper. In our simulations, we choose $\delta t = 15dt = 1.5 \cdot 10^{-2}$, and we initialize using the constrained runs scheme with 10 steps.

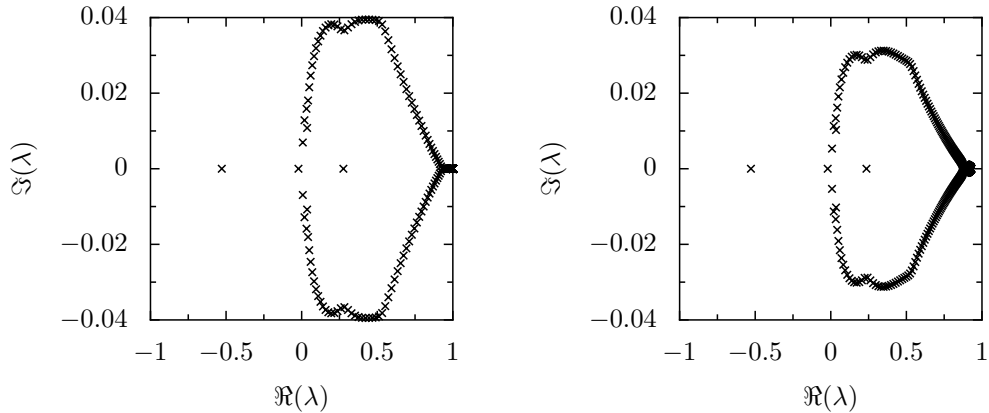


Figure 5: Fisher traveling wave problem. Left: Spectrum of the system matrix of equation (31). Right: spectrum of the preconditioning matrix (36).

6.1.2 Performance of the preconditioner

We now compute the spectrum of the matrix $A(\bar{U}^{(0)}, \delta t)$, using the parameters defined above. To this end, we construct the matrix $A(\bar{U}^{(0)}, \delta t)$ explicitly by computing the matrix-vector products with all coordinate vectors $e_i = [0, \dots, 0, 1, 0, \dots, 0]^T$. The matrix-vector products are estimated using (32) with $\epsilon = 1 \cdot 10^{-8}$. The results are shown in figure 5(left). We compare with the spectrum of the matrix $M(U^{(0)}, \delta t)$ shown in figure 5(right). We see good agreement between the two spectra. The differences are in the imaginary part of the eigenvalues, and in the very fast modes, which show up around 1 since we are computing the spectrum of the fixed point iteration. Also remark how the zero eigenvalue, corresponding to the singularity of the fixed point equation (28), is split into two isolated eigenvalues by the addition of the phase condition and the artificial unknown α .

The spectrum of the matrix $M(\bar{U}^{(0)}, \delta t)^{-1}A(\bar{U}^{(0)}, \delta t)$ is shown in figure 6(left). We see that this spectrum is nicely clustered around 1. As a result, we obtain very fast GMRES convergence. Figure 6 shows the error as a function of the number of GMRES iterations. We clearly see the fast linear convergence, as predicted by the theory [31].

6.1.3 Convergence of the Newton process

We are now ready to show the convergence of the Newton process. To this end, we take as an initial guess $\bar{U}^{(0)}$ a smoothed step function of the form

$$\bar{U}^{(0)} = \frac{1}{\exp(2(x - L/2)) + 1}, \quad (40)$$

with $L = 10$, the length of the interval. The convergence of the Newton process is shown in figure 7. We notice that the convergence is linear, and the convergence factor changes after approximately 4 iterations. In the process, we have converged to the traveling wave

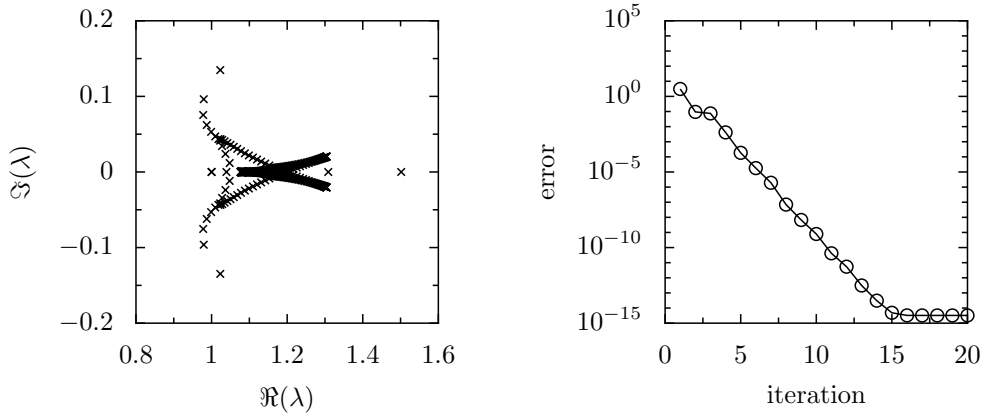


Figure 6: Fisher traveling wave problem. Left: spectrum of the product of the inverse of the preconditioner and the system matrix. Right: error of the linear system as a function of the number of GMRES iterations.

solution shown in figure 1, and $\alpha^* = -2.24 \cdot 10^{-4}$. The fact that α^* is not equal to zero can be shown to be an artifact of the space discretization, combined with the truncation to a finite domain. Indeed, α^* becomes smaller when we refine the lattice Boltzmann grid (and decrease the time-step to keep ω fixed). We can explain this as follows: the conclusion that α^* should equal zero follows from the assumption that the extra column that is added in the Jacobian, $d_\zeta \bar{U}$, is the eigenvector associated with the zero eigenvalue of the fixed point map (28). However, due to the space discretization, $d_\zeta \bar{U}$ will only be an *approximation* to this eigenvector. Therefore, we are using a quasi-Newton method (hence the linear convergence), and the solution value α^* will be non-zero but small. The convergence factor changes when the traveling wave solution has been computed to machine precision. At that point, only the error in α shows up in the residual, indicating that the non-zero value of α^* is indeed the main cause for the non-quadratic convergence.

6.2 Planar streamer front

As a second example, we numerically study model problem 3.2 for planar ionization fronts on the domain $[0, 130]$ with grid parameter $dx = 1 \cdot 10^{-1}$ and $dt = 1 \cdot 10^{-3}$. We choose the diffusion coefficient to be $a = 1$ and the electric field $E_\infty^+ = -1$ (i.e. a constant, large electric field on the far right). For these parameters, the corresponding lattice Boltzmann relaxation parameter is $\omega \approx 1.538$, and $N = 1300$, which implies that the unknown solution has 2601 unknowns. We intend to compute the traveling wave solution with the minimal speed $c^* = |E_\infty^+| + 2\sqrt{Dg(E_\infty^+)}$, which is depicted in figure 2. The initial guess $U^{(0)}$ for the Newton process is obtained by a time integration of the ionization PDE (23) over a time interval of size $4000dt$ with initial condition

$$U(x, 0) = \rho(x, 0) = \exp(-15x^2), x \in [0, 130]. \quad (41)$$

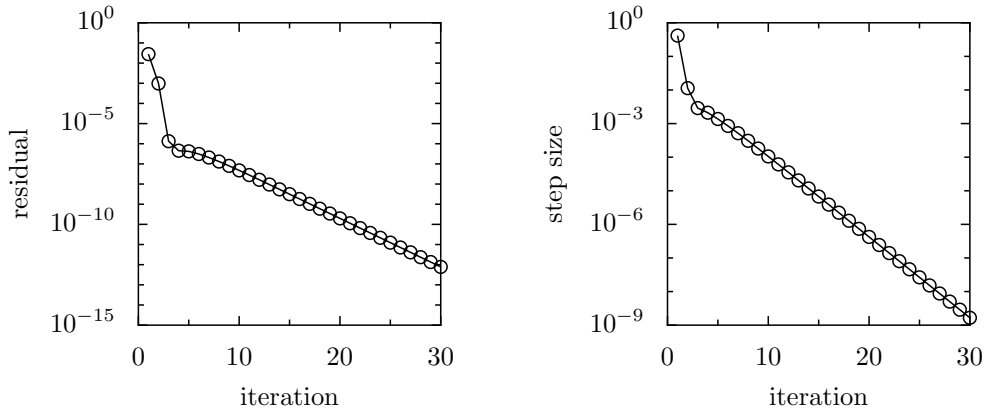


Figure 7: Fisher traveling wave problem. Convergence of the Newton process as a function of iteration number.

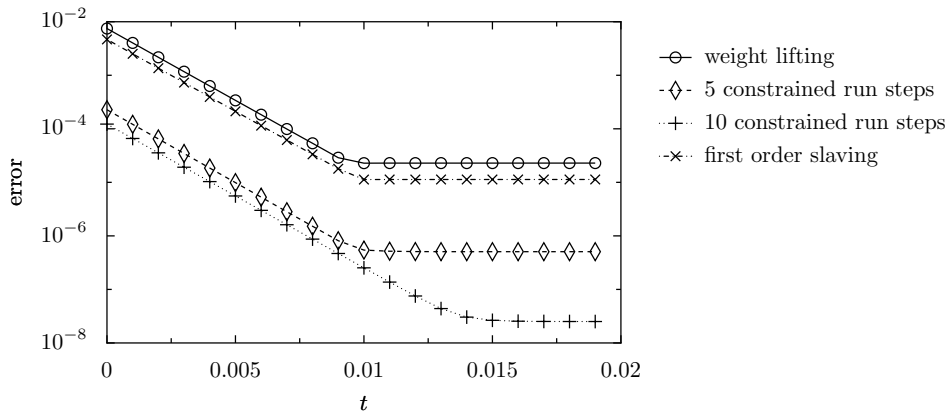


Figure 8: Evolution of the initialization error for the planar streamer model with different lifting procedures. We show the difference between the distribution function of the re-initialized and the original lattice Boltzmann simulation.

6.2.1 Initialization

Again, we study the properties of the initialization by comparing the exact evolution of a lattice Boltzmann simulation with the evolution after re-initialization. We performed a simulation of 100 steps, starting from $\bar{U}^{(0)}$, with the lattice Boltzmann model (22), which is initialized using the first order slaving relations. Again, we extract the density at time $t = 80dt$, and initialize a second lattice Boltzmann simulation using the three procedures described in section 4.1. We observe the same behaviour as for the Fisher model. In figure 8, we show the evolution of the initialization error during the first 20 steps after re-initialization. We again see an initial convergence towards the exact solution, which stagnates after 10 to 20 time-steps. Depending on the accuracy of the lifting step, we get a better correspondence with the correct distribution functions.

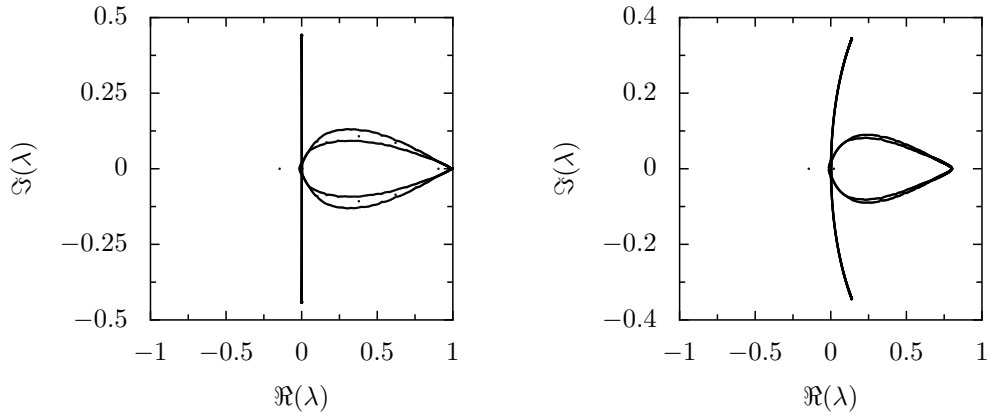


Figure 9: The planar streamer front problem. Left: Spectrum of the system matrix of equation (31). Right: spectrum of the preconditioner (36).

Based on these observations, we choose $\delta t = 15dt = 1.5 \cdot 10^{-2}$ in our simulations, and we initialize using the constrained runs scheme with 10 steps.

6.2.2 Performance of the preconditioner

In figure 9, we show the spectrum of the matrix $A(\bar{U}^{(0)}, \delta t)$, using the parameters defined above, and the spectrum of the corresponding preconditioning matrix $M(\bar{U}^{(0)}, \delta t)$. Again, we see good qualitative agreement between the two spectra, but the differences are more pronounced than for the Fisher equation.

The spectrum of the matrix $M(\bar{U}^{(0)}, \delta t)^{-1}A(\bar{U}^{(0)}, \delta t)$ is shown in figure 10(left). Although most eigenvalues are in a small cluster around 1, a few eigenvalues are scattered on the real axis. These additional eigenvalues result in a temporary stagnation of the GMRES convergence, as shown in figure 10 (right). Between these stagnations, linear convergence is observed. We note that, even with the temporary stagnation, the solution is computed in 30 to 40 iterations, while the number of unknowns is 2601.

6.2.3 Convergence of the Newton process

We proceed to show the convergence of the Newton process, starting from the initial guess $\bar{U}^{(0)}$. The results are shown in figure 11. We plot the norm of the residual and the correction $(d\bar{U}^{(k)}, \alpha^{(k)})$ after each iteration. For this problem, we get quadratic convergence towards the solutions shown in figure 2, and $\alpha^* = 0$. Thus, in this case, the effect of the discretization is much less pronounced, or even absent.

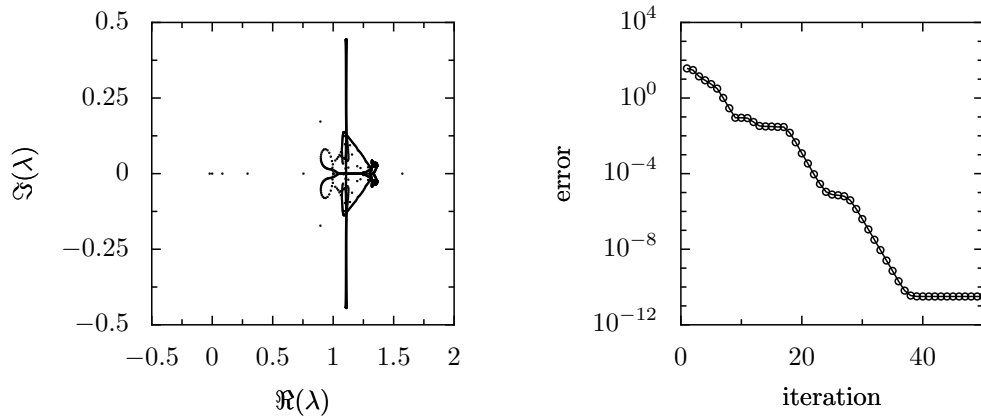


Figure 10: Planar streamer front problem. Left: spectrum of the preconditioned system matrix $M^{-1}A$ (equation (33)) for the first Newton step. Right: the convergence of the preconditioned GMRES procedure as a function of the number of iterations.

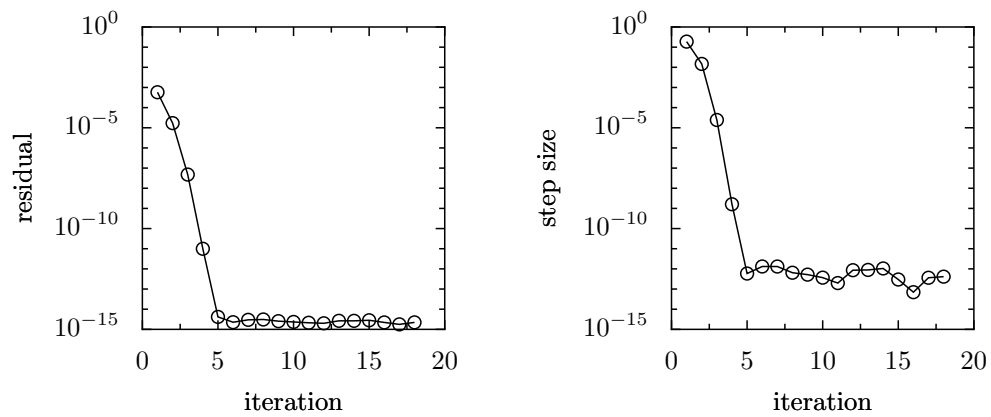


Figure 11: Planar streamer front problem. Convergence of the Newton process as a function of iteration number.

7 Discussion and conclusions

In this article, we showed how one can use a coarse-grained time-stepper to compute traveling wave solutions of lattice Boltzmann models. In a co-moving frame, emulated by performing a shift-back operation after each coarse-grained time-step, the traveling wave appears as a steady state, which is computed using a Jacobian-free Newton–GMRES method. The method uses repeated calls to the coarse-grained time-stepper to estimate the required matrix-vector products. For efficiency reasons, we limited the size of the coarse-grained time-step δt . The real part of the spectrum of the resulting Jacobian ranges from 0 to 1, which results in slow convergence of Krylov methods. Therefore, we accelerated convergence of the GMRES procedure by introducing a preconditioner that is based on an approximate macroscopic model, which is derived from the lattice Boltzmann model using a Chapman–Enskog expansion. We illustrated the approach on a lattice Boltzmann model for the Fisher equation and on a model for an ionization wave.

The total cost of finding a solution is determined by the required number of microscopic time-steps, which depends on the number of GMRES iterations and on the number of microscopic time-steps per matrix-vector product. For each matrix-vector product, we use the microscopic time-stepper both during the simulation and the lifting step when the constrained runs scheme is used. The required number of calls to the microscopic time-stepper is determined by the microscopic relaxation parameter ω , since the convergence rate of the distribution functions towards their correctly slaved values is given by $|1 - \omega|$. In our examples, approximately 10 lattice Boltzmann time-steps were needed for each lifting operation and an additional 10 to 15 for each microscopic simulation.

The convergence rate of the GMRES method is closely related to the quality of the preconditioner. The preconditioner performs well when the approximate macroscopic model is a good approximation of the lattice Boltzmann model. Our experiments indicate that the quality of the preconditioner is not related to the number of lattice points N , which implies that the number of GMRES iterations is approximately constant with varying N .

Since the number of time-steps only depends on the relaxation parameter ω and the spectrum of the preconditioned time-stepper, we conclude that the convergence rate is independent of the number of variables in the problem. As a consequence, the algorithm scales with the cost of taking a single lattice Boltzmann time-step and the cost of a direct solve with the preconditioning matrix.

In our numerical examples we found that, on average, 2000 time-steps are required to converge to the traveling wave solution. This is still expensive if we compare with straightforward time integration. E.g. for the Fisher model, a localized initial state evolves into a steady traveling wave within 9000 time-steps. However, direct time integration loses its appeal in situations where the microscopic time-step is so small that it is computationally infeasible to reach the time horizon where the traveling wave becomes steady. Furthermore,

the total number of time-steps will be much smaller in the context of continuation, where the behaviour of the solutions is studied as a function of one or more varying parameters. In this setting, the solution for nearby parameter values provides an accurate initial guess, hereby lowering the required number of Newton steps. Also, the Newton–GMRES method allows us to find *unstable* traveling waves. These will never be found by simulation, since any perturbation will grow, and will destroy the traveling wave.

Note that preconditioning with a roughly approximate macroscopic PDE model can also be helpful to study the linear stability properties of the traveling wave. Indeed, the relevant rightmost eigenvalues of the Jacobian matrix in the solution can be computed by an Arnoldi iteration that requires the solution of a linear system in each iteration [21]. This linear system can again be preconditioned with the techniques proposed in this article.

In principle, the Newton–GMRES method could be applied to the lattice Boltzmann model directly. However, it is much harder to find an appropriate preconditioner in that setting. Indeed, one cannot expect a preconditioner based on the approximate PDE to work well, since the fast time-scales, which describe the slaving of the higher order moments, will not be correctly accounted for. We also emphasize that, from the coarse-grained solution, the detailed solution can easily be reconstructed using the constrained runs lifting scheme. Our method generalizes readily to lattice Boltzmann models with a more detailed description of the velocity space. A particular five-speed model, in which the Townsend approximation for the reaction term is replaced by a more realistic set of microscopic interaction rules, is currently being investigated [43].

Acknowledgements

The authors thank Pieter Van Leemput, Christophe Vandekerckhove, Kurt Lust and Tim Boonen for interesting discussions about various aspects of this work. Pieter Van Leemput provided us with figure 3. GS is a Research Assistant of the Fund for Scientific Research – Flanders. WV is supported by the Belgian Science Policy Office through its action “return grants”. This work was supported by the Fund for Scientific Research – Flanders through Research Project G.0130.03 (GS, DR, WV) and by the Interuniversity Attraction Poles Programme of the Belgian Science Policy Office through grant IUAP/V/22. The scientific responsibility rests with its authors. The research of IGK was partially supported by the US DOE and DARPA.

References

- [1] P.L. Bhatnagar, E.P. Gross, and M. Krook. A model for collision processes in gases, I. Small amplitude processes in charged and neutral one-component systems. *Physical Review*, 94(3):511–525, 1954.

- [2] L. Boltzmann. *Lectures on gas theory*. University of California Press, Berkeley, 1964.
- [3] S. Chandrasekaran and M. Gu. Fast and stable algorithms for banded plus semiseparable systems of linear equations. *SIAM Journal on Matrix Analysis and Applications*, 25(2):373–384, 2003.
- [4] B. Chopard, A. Dupuis, A. Masselot, and P. Luthi. Cellular automata and lattice Boltzmann techniques: an approach to model and simulate complex systems. *Advances in Complex Systems*, 5:103–246, 2002.
- [5] S.P. Dawson, S. Chen, and G.D. Doolen. Lattice Boltzmann computations for reaction-diffusion equations. *Journal of Chemical Physics*, 98(2):1514–1523, 1993.
- [6] E. Doedel. Auto: a package for the automatic bifurcation analysis of autonomous systems. *Cong. Numer.*, pages 265–384, 1981.
- [7] E.J. Doedel, H. B. Keller, and J. P. Kernévez. Numerical analysis and control of bifurcation problems, part I. *International Journal of Bifurcation and Chaos*, 3:493–520, 1991.
- [8] E.J. Doedel, H. B. Keller, and J. P. Kernévez. Numerical analysis and control of bifurcation problems, part II. *International Journal of Bifurcation and Chaos*, 4:745–772, 1991.
- [9] U. Ebert, W. van Saarloos, and C. Caroli. Propagation and structure of planar streamer fronts. *Phys. Rev. E*, 55:1530 – 1549, 1997.
- [10] K. Engelborghs, T. Luzyanina, and G. Samaey. DDE-BIFTOOL v. 2.00: a Matlab package for bifurcation analysis of delay differential equations. Report TW 330, Department of Computer Science, K.U.Leuven, Leuven, Belgium, October 2001.
- [11] R.A. Fisher. The wave of advance of advantageous genes. *Annals of Eugenics*, 7:353–369, 1937.
- [12] C.W. Gear, T.J. Kaper, I.G. Kevrekidis, and A. Zagaris. Projecting to a slow manifold: Singularly perturbed systems and legacy codes. *SIAM Journal on Applied Dynamical Systems*, 4(3), 2005.
- [13] C.W. Gear and I.G. Kevrekidis. Constraint-defined manifolds: a legacy code approach to low-dimensional computation. *J. Sci. Comp.*, 2004. In press.
- [14] C.W. Gear, I.G. Kevrekidis, and C. Theodoropoulos. Coarse integration/bifurcation analysis via microscopic simulators: micro-Galerkin methods. *Computers and Chemical Engineering*, 26:941–963, 2002.

- [15] A.N. Gorban and I.V. Karlin. *Invariant manifolds for physical and chemical kinetics*, volume 660 of *Lecture Notes in Physics*. Springer–Verlag Berlin Heidelberg, 2005.
- [16] X. He and L.-S. Luo. A priori derivation of the lattice Boltzmann equation. *Physical Review E*, 55(6):R6333–R6336, 1997.
- [17] G. Hummer and I.G. Kevrekidis. Coarse molecular dynamics of a peptide fragment: free energy, kinetics and long-time dynamics computations. *J. Chem. Phys.*, 118(23):10762–10773, 2003. Can be obtained as physics/0212108 at arxiv.org.
- [18] C.T. Kelley, I.G. Kevrekidis, and L. Qiao. Newton–Krylov solvers for time-steppers. Can be obtained as math/0404374 from <http://www.arxiv.org>, 2004.
- [19] I.G. Kevrekidis, C.W. Gear, J.M. Hyman, P.G. Kevrekidis, O. Runborg, and C. Theodoropoulos. Equation-free, coarse-grained multiscale computation: enabling microscopic simulators to perform system-level tasks. *Comm. Math. Sciences*, 1(4):715–762, 2003.
- [20] D.A. Knoll and D.E. Keyes. Jacobian-free newton–krylov methods: a survey of approaches and applications. *Journal of Computational Physics*, 193:357–397, 2004.
- [21] R.B. Lehoucq and A.G. Salinger. Large-scale eigenvalue calculations for stability analysis of steady flows on massively parallel computers. *International Journal for Numerical Methods in Fluids*, 36:309–327, 2001.
- [22] R. Liboff. *Kinetic theory: classical, quantum and relativistic descriptions*. Springer–Verlag New York, 2003.
- [23] Li-Shi Luo. Unified theory of lattice boltzmann models for nonideal gases. *Phys. Rev. Lett.*, 81:1618, 1998.
- [24] K. Lust. *Numerical bifurcation analysis of periodic solutions of partial differential equations*. PhD thesis, Katholieke Universiteit Leuven, 1997.
- [25] K. Lust. Private communication, 2005.
- [26] K. Lust, D. Roose, A. Spence, and A.R. Champneys. An adaptive Newton–Picard algorithm with subspace iteration for computing periodic solutions. *SIAM Journal on Scientific Computing*, 19(4):1188–1209, 1998.
- [27] A.G. Makeev, D. Maroudas, A.Z. Panagiotopoulos, and I.G. Kevrekidis. Coarse bifurcation analysis of kinetic Monte Carlo simulations: a lattice-gas model with lateral interactions. *J. Chem. Phys.*, 117(18):8229–8240, 2002.
- [28] J.D. Murray. *Mathematical biology*. Springer–Verlag, 1989.

- [29] Y.H. Qian and S.A. Orszag. Scalings in diffusion-driven reaction $A+B \rightarrow C$: numerical simulations by lattice BGK models. *Journal of Statistical Physics*, 81:237–253, 1995.
- [30] J. P. Ryckaert, G. Ciccotti, and H. Berendsen. Numerical integration of the cartesian equation of motion of a system with constraints: molecular dynamics of n-alkanes. *J. Comp. Phys.*, 23:237, 1977.
- [31] Y. Saad. *Iterative Methods for Sparse Linear Systems*. Society for Industrial and Applied Mathematics, Philadelphia, PA, USA, 2003.
- [32] Y. Saad and M.H. Schultz. GMRES: A generalized minimal residual algorithm for solving nonsymmetric linear systems. *SIAM Journal of Scientific and Statistical Computing*, 7(3):856–869, 1986.
- [33] D.S. Schmidt. Hopf’s bifurcation theorem and the center theorems of Lyapunov. In J.E. Marsden and M. McCracken, editors, *The Hopf bifurcation and its applications*, volume 19 of *Applied Math. Sci.*, pages 95–104. Springer, New York, 1976.
- [34] G.M. Schroff and H.B. Keller. Stabilization of unstable procedures: the recursive projection method. *SIAM Journal on Numerical Analysis*, 30:1099–1120, 1993.
- [35] C.I. Siettos, A. Armaou, A.G. Makeev, and I.G. Kevrekidis. Microscopic/stochastic timesteppers and coarse control: a kinetic Monte Carlo example. *AIChE J.*, 49(7):1922–1926, 2003. Can be obtained as nlin.CG/0207017 at arxiv.org.
- [36] C.I. Siettos, M.D. Graham, and I.G. Kevrekidis. Coarse Brownian dynamics for nematic liquid crystals: bifurcation, projective integration and control via stochastic simulation. *J. Chem. Phys.*, 118(22):10149–10157, 2003. Can be obtained as cond-mat/0211455 at arxiv.org.
- [37] S. Succi. *The lattice Boltzmann equation for fluid dynamics and beyond*. Oxford Science Publications, 2001.
- [38] C. Theodoropoulos, Y.H. Qian, and I.G. Kevrekidis. Coarse stability and bifurcation analysis using time-steppers: a reaction-diffusion example. In *Proc. Natl. Acad. Sci.*, volume 97, pages 9840–9845, 2000.
- [39] G. M. Torrie and J. P. Valleau. Monte carlo free energy estimation using non-boltzmann sampling: application to the sub-critical lennard jones fluid. *Chem. Phys. Letters*, 28:578–581, 1974.
- [40] P. Van Leemput, K. Lust, and I.G. Kevrekidis. Coarse-grained numerical bifurcation analysis of lattice Boltzmann models. *Physica D*, 210(1–2):58–76, 2005.
- [41] P. Van Leemput, W. Vanroose, and D. Roose. Initialization of a lattice Boltzmann model with constrained runs. *Journal of Computational Physics*, 2005. Submitted.

- [42] P. Van Leemput, W. Vanroose, and D. Roose. Numerical and analytical spatial coupling of a lattice Boltzmann model and a partial differential equation. In A.N. Gorban et al., editor, *Model Reduction and Coarse-graining Approaches for Multiscale Phenomena*, Springer Lecture Series. Springer, 2006.
- [43] W. Vanroose, G. Samaey, P. Van Leemput, and D. Roose. Analysis of a lattice Boltzmann model for planar streamer fronts. In preparation, 2006.
- [44] K. Xu. Gas-kinetic schemes for unsteady compressible flow simulations. VKI (von Karman Institute) Lecture Series 1998-03, 1998.